H2S interaction with HKUST-1 and ZIF-8 MOFs: A multitechnique study

UNIVERSITÀ DEGLI STUDI DI TORINO

H_2S interaction with HKUST-1 and ZIF-8 MOFs: A multitechnique study

by

Jayashree Ethiraj, Francesca Bonino, Carlo Lamberti, Silvia Bordiga

Microporous Mesoporous Mater., **207** (2015) 90-94

doi: 10.1016/j.micromeso.2014.12.034

H_2S interaction with HKUST-1 and ZIF-8 MOFs: a multitechnique study

Jayashree Ethiraj,[1] Francesca Bonino,[1*] Carlo Lamberti,[1,2] Silvia Bordiga[1]

[1]Department of Chemistry, NIS and INSTM Reference Centre, University of Turin, Via G. Quarello 15, I-10135 and Via P. Giuria 7, I-10125, Turin, Italy

[2] Southern Federal University, Zorge street 5, 344090 Rostov-on-Don, Russia

[*] Corresponding author: francesca.bonino@unito.it

Abstract

The interaction of H_2S with HKUST-1 and ZIF-8 MOFs has been studied by means of FT-IR, Raman, DRUV-Vis-NIR and PXRD techniques. At very low equilibrium pressure (below 5mbar) a stepwise structural distortion is observed in both HKUST-1 and ZIF-8. At higher equilibrium pressures 20-60 mbar, in particular PXRD technique, showed the structural destruction of HKUST-1 with formation of a covallite (CuS) phase and some structural distortion of ZIF-8.

KeyWords : Metal-organic frameworks • Hydrogen Sulfide • IR spectroscopy • Raman spectroscopy • X-ray diffraction

1. Introduction

Hydrogen sulphide (H_2S) is a colourless, toxic and flammable gas, that needs to be removed from gas mixtures used in the energy sector as it acts as poison in respect of most of the precious metal catalysts. At the present time both physical and chemical absorption media use aqueous solvents like amine solutions (monoethanolamine (MEA), diethanolamine (DEA) and methyldiethanolamine (MDEA)), potassium carbonate solution, alkaline activated carbons, zeolites.[1-3] Metal-organic frameworks (MOFs), known for their high porosity and structural flexibility,[4-5] have shown reversible adsorption towards H_2S gas. Some of the well studied MOFs are MIL-53(Al, Cr, Fe), MIL-47(V), MIL-100(Cr), and MIL-101(Cr) [6-8] and CPO-27-Ni [9]. MOFs comprising a

tridimensional succession of motifs, with metal ions in 2+/3+/4+ states, have been found to be stable in the presence of water or humidity and they exhibit a high sulphur selectivity and strong chemical resistance to the corrosive sulfur gases; and can be regenerated without high energetic regeneration costs. [10]

HKUST-1, first reported in 1999 is a well studied material [11] where Cu^{2+} ions form dimers, each copper atom is coordinated by four oxygens of the benzene-1,3,5-tricarboxilate (BTC) linkers and by one water molecule. Single-crystal data have shown that it forms face centered cubic crystals that contains a large square-shaped pores (9.9 Å). The presence of water molecule in the first coordination sphere of copper ions can be removed by dehydration creating coordinative vacancy on Cu^{2+} species. The coordinative unsaturation of metal centers after thermal treatments and interaction with probe molecules like NO, CO_2, CO, N_2 and H_2 have reported in refs. [12-14]. Moreover, HKUST-1 has been well studied for other gases like ammonia.[15] The interaction of small molecules with the coordinatively unsatured metal centers of the HKUST-1 by means of density functional theory have been studied for CO, CO_2, OCS, SO_2, NO, NO_2, N_2O, NH_3, PH_3 and other small molecules.[16] Some experimental evidence of H_2S interaction with HKUST-1 is reported by Petit et al., where they have proposed a mechanism of degradation of HKUST-1 upon H_2S adsorption. [17-19] On the other hand, Gutierrez-Sevillano et. al [20] have studied H_2S adsorption on three well known MOFs, namely HKUST-1, MIL-47(V), and IRMOF-1(Zn). According to their study, the H_2S adsorption energy in the case of HKUST-1, is -43.4 (kJ mol^{-1}) which is lower than H_2O adsorption energy of -46.7(kJ mol^{-1}) and they claim that there must be something missing in the mechanisms proposed so far to explain the degradation observed in the MOF upon adsorption of H_2S. Theoretical studies on CPO-27-Ni have also shown higher interaction energy for H_2O than H_2S. [9]

The second MOF of this study, ZIF-8 (Zeolitic Imidazolate Framework) [21-22] is porous and crystalline framework in which the tetrahedral metal ions are linked by imidazolate (Im) units. ZIF structures may be compared with those of zeolites, as the bridging angle formed by this linkage is

analogous to that between silicon oxygen and aluminum oxygen units in zeolites. ZIF-8 as a promising storage material was investigated at high pressures up to ~39 GPa by in situ FTIR spectroscopy.[23] Apart from characterization, nanosized ZIF-8 has been studied and proved to be a reusable esterification catalyst[24] and the latest study on functionalization of ZIF-8 by using malonitrile has been reported for H_2S fluorescent detection and highly selective amino acid recognition.[25]

In the present contribution we report a multitechnique study (FT-IR, Raman, DRUV-Vis-NIR, PXRD) on the H_2S interaction with HKUST-1 and ZIF-8. Based on our experience, the multitechnical approach is very useful in the characterization of complex materials such as MOFs. [26-28]

2. Experimental

MOF samples, HKUST-1(Basolite^{TM} C300) and ZIF-8 (Basolite^{TM} Z1200) were purchased by Sigma-Aldrich. The samples were activated in vacuo at 423K and 573K respectively.

FT-IR spectra were collected on a Nicolet-6700 spectrometer equipped with a MCT B type detector, in the range of 4000-400 cm^{-1}, in transmission mode with a 2 cm^{-1} resolution. The samples have been prepared as self-supported thin pellets.

UV-Vis-NIR spectra have been collected in Diffuse Reflectance mode on a Cary5000 Varian spectrophotometer equipped with a reflectance sphere. All the samples have been measured in powder form in a suprasil quartz homemade optical bulb cell which allows measurement in controlled atmosphere.

Raman spectra were recorded on a Renishaw inVia Raman microscope spectrometer. Unfortunately the two samples revealed a different fluorescence behavior depending on the laser line and therefore two different laser lines were used. In particular an Ar^+ laser emitting at 514 nm and a diode laser emitting at 785 nm were used for HKUST-1 and ZIF-8 respectively. Photons scattered by the sample were dispersed by a 1800 (514 nm) and 1200 (785 nm) lines/mm grating monochromator

and were simultaneously collected on a CCD camera; the collection optic was set at 20X objective. The spectral collection setup consisted of 50 acquisitions, each of 10 sec.

X-ray Powder Diffraction (PXRD) patterns have been collected with a PW3050/60 X'Pert PRO MPD diffractometer from PANalytical working in Debye–Scherrer geometry, using a high power ceramic tube PW3373/10 LFF with a Cu anode equipped with Ni filter to attenuate K_β and focused by X-ray mirror PW3152/63. Scattered photons have been collected by a RTMS (Real Time Multiple Strip) X'celerator detector. The samples have been measured as powders inside a 0.8 mm boronsilicate capillary in air.

3.Results and Discussion

3.1. FT-IR spectroscopy

3.1.1 Activation of the samples[26]

Figure 1a shows FT-IR spectra of HKUST-1 in air and activated at 423K for 1h. The spectrum of the hydrated sample is clearly dominated by large amount of solvent in the 3800-2000 cm^{-1} region. In the dehydrated form IR absorption bands of the BTC linker are observed in 1800-400 cm^{-1} range.[12] The out of scale absorption bands in the range 1700-1500 cm^{-1} and 1500-1300 cm^{-1} correspond to $\nu_{asym}(C\text{-}O_2)$ and $\nu_{sym}(C\text{-}O_2)$.[12-15] The other very intense absorption band is centered at 738cm^{-1} and it was previously assigned[12-15]to ν(C-H) bending mode. In the considered range only the band centered at 505 cm^{-1} is assigned to a vibrational mode directly involving the Cu centre. Following the previous interpretations,[12-15] this feature is assigned to Cu−O stretching mode.

Figure 1b shows ZIF-8 in air and activated at 573K for 2h. Solvent used in the synthesis (DMF) and water are easily removed upon thermal activation in vacuo. The broad band centered at 3000 cm^{-1} due to the presence of some hydrogen bond between MOF functional groups with solvent disappears, while ZIF-8 fingerprint vibrational modes become clearly distinguishable. At higher frequency the activated ZIF-8 shows two contributions: the first one centered at 3134 cm^{-1} and the

second one in the 3000-2850 cm^{-1} range, ascribable to C-H stretching vibrational modes respectively of the ring and of the methyl group present in the 2-methylimidazole linker. The peak at 1586 cm^{-1} can be assigned as the C=N stretch mode specifically, whereas the intense and convoluted bands at 1500–1350 cm^{-1} are associated with the entire ring stretching.[23] The bands in the spectral region of 1350-900 cm^{-1} are for the in-plane bending of the ring while those below 800 cm^{-1} are assigned as out-of-plane bending.[23] As expected, clearly, a very intense band at 421 cm^{-1} due to Zn–N stretching mode is clearly observed.[23]

3.1.2 H_2S adsoprtion on HKUST-1 and ZIF-8

FT-IR spectra of HKUST-1 contacted, after activation, with increasing dosages of H_2S (up to p_{eq}= 10 mbar) are reported in Figure 2a. Surprisingly, and differently from the CPO-27-Ni case[9], the three IR active vibrational modes of molecular H_2S at 2626, 2614, and 1182 cm^{-1}, corresponding to the asymmetric, symmetric stretching, and bending vibrational modes, are totally absent. The interaction results in a progressive growing up of very broad and indefinite bands, in the 3700-2100, 1750-1100 and 950-650 cm^{-1} range. Moreover the band at 505 cm^{-1} due to the Cu-O vibrational mode[12-15] is gradually eroded. All these evidences are the first signal of a probable HKUST-1 framework instability upon interaction with H_2S.

In the case of ZIF-8 (Figure 2b), H_2S dosage is stopped at p_{eq}= 5 mbar (dark yellow curve), due to the extreme fragility of the pellet at higher adsorbate pressures. Very differently to HKUST-1, all the vibrational modes in the low frequency range (1700-400 cm^{-1}) are unperturbed. However, again H_2S vibrational modes are hardly recognized and in the higher frequency range (3500-2550 cm^{-1}), less markedly than in HKUST-1 case, broad bands appear, overlapping ZIF-8 vibrational fingerprints. This fact can be probably simply due to the presence of hydrogen bonded species and not to the MOF decomposition (at least this is the evidence at this coverage by means of IR spectroscopy).

3.2 Raman spectroscopy

Vibrational Raman spectra (in the 1700-150 cm^{-1} range) of both HKUST-1 and ZIF-8 have also been acquired (Figure 3). Part a) reports the Raman spectra of as such (cyan curve), activated (blue curve) and interacting with H_2S (olive curves) HKUST-1. As previously reported, the as such sample spectrum is dominated by the organic linker contribution. The bands at 1610 cm^{-1} and 1004 cm^{-1} are associated with ν(C=C) modes of the benzene ring; the peaks at 828 cm^{-1} and 742 cm^{-1} are ascribed to out-of-plane ring (C-H) bending vibrations and to out-of-plane ring bending, respectively. The bands at 1536 cm^{-1} and 1452 cm^{-1} are due to the $\nu_{asym}(C\text{-}O_2)$ and $\nu_{sym}(C\text{-}O_2)$ units. The bands at 496 cm^{-1}, 280 cm^{-1} and 190 cm^{-1} correspond to vibrational modes directly involving Cu(II) species. Unfortunately, activation leads to deterioration of the signal to noise ratio of the measured spectrum. However, while the dehydration process of HKUST-1 MOF does not affect the high-frequency modes of the organic part of the framework, it is evident that the modes in the 600-150 cm^{-1} range, ascribed to vibrational modes involving Cu(II) species, are dramatically perturbed by water removal. In particular the band at 496 cm^{-1} shifts to 508 cm^{-1} and a peak at 224 cm^{-1} appears. These two contributions are assigned respectively to Cu-O and Cu-Cu vibrational modes.[12-15] Progressive dosages of H_2S cause almost the total disappearance of all the HKUST-1 bands and the growing of a new very broad band centered at 415 cm^{-1}. It is quite evident, more than in the case of IR technique, that, upon interaction with H_2S, HKUST-1 loses all its fingerprint vibrational modes and a new Cu-S species, responsible for the appearance of the band at lower frequency,[29] is formed.

Part b) of Figure 3 reports Raman spectra of ZIF-8. The sample in air (grey curve) shows the typical Raman fingerprint of ZIF-8. Very strong bands were observed at 173 cm^{-1}, 686 cm^{-1}, 1149 cm^{-1}, and 1463 cm^{-1} corresponding to Zn−N stretching, imidazole ring puckering, C5−N stretching and methyl bending, respectively.[30] Unfortunately, in this case, it is not possible to study the vibrational perturbations upon H_2S dosages, as already the activated sample gives very strong fluorescence covering all the possible Raman signals in the considered range.

3.3 DRUV-Vis-NIR spectroscopy

As previously reported by us[12-15] HKUST-1, upon activation changes drastically its colour from light cyan to blue navy. After interaction with H_2S the sample turns to dark green colour (see Figure 4a1).

This trend can be explained only if a change in the coordination sphere of copper is invoked, as the colour is associated with d−d transitions of Cu(II) ions (see Figure 4a2).

The spectrum of the sample in air (cyan curve) shows the already known features, that are (i) an edge around 350 nm due to a ligand to metal charge transfer (LMCT) transition from oxygen to copper atoms and (ii) a band centred at 708 nm, characteristic of the d−d transition for Cu(II) species in a distorted octahedral local geometry. Upon activation at 423 K (blue curve), a shoulder in the d−d band centred at 609 nm, a red shift of the maximum, previously observed at 708 nm, to 719 nm and of the absorption associated with the LMCT transition are observed. The change in the d−d region is ascribed to the activation of new available d−d transitions due to a loss of degeneracy in d levels produced by a change in the symmetry around copper. The LMCT edge shift is explained as a consequence of the change of (i) the hydration conditions of the carboxylated group and (ii) the coordination sphere of copper ions.

Upon a small dosage of H_2S (grey curve), the octahedral geometry is perturbed and the spectrum goes back to that observed in case of sample in air with a strong decrease in the intensity of the band at 708nm. When the interaction occurs with 20 mbar of H_2S the LMCT shifts to 470nm and the d-d band blue-shifts to 687, with significant decrease in intensity . These experimental evidences, again, show that the coordination sphere of copper is strongly perturbed upon H_2S interaction.

Moving now to ZIF-8, the sample, upon H_2S interaction, changes only slightly colour, from white to very pale yellow (see Figure 4b1). Thus, DRUV-Vis spectra of ZIF-8 (Figure 4b2) interactiong with H_2S (dark yellow curve) are less informative than in the previous case. In fact the spectrum is almost superimposed to that one of the activated sample (black curve). Also the passage from the

sample in air (grey curve) to the activated form reveals small differences. In particular, upon activation, besides the very intense band with edge at 240nm, due to electronic transitions involving the linker itself or LMCT from the linker nitrogen atoms to zinc atoms, a new small multi-component contribution appears centred at 400 nm.

3.4 Powder X-ray Diffraction

As expected from previous results, upon H_2S dosage, HKUST-1 x-ray diffraction pattern is completely destroyed and new well defined reflections (blue full circle symbols) appear (see Figure 5a). Looking at literature data[31] they can be easily assigned to covellite CuS. This is the final proof that H_2S is reacting with copper centres, forming a new compound, that is covellite, and demolishing HKUST-1 framework.

In case of ZIF-8, the effect of H_2S interaction, is very less destructive, even at pressure higher than for HKUST-1 (see Figure 5b). A small number of new reflections (orange full circle symbols) appear at low angles (see the inset). Unfortunately their assignment is not straightforward and they do not correspond to any sulphide phase involving zinc.

4. Conclusions

HKUST-1 and ZIF-8 interacting with H_2S have been characterized by means of FTIR, Raman, DRUV-Vis and PXRD techniques.

HKUST-1 clearly showed a strong perturbation of all the vibrational, electronic and structural fingerprints due to the formation of a covellite CuS phase and consequent destruction of the framework. On the contrary, ZIF-8 revealed to be more stable, undergoing only to a slight framework perturbation. In this case PXRD technique showed the presence of new small reflections, not ascribable to any sulphide involving zinc atom.

Acknowledgements

This work has been supported by EU FP-7 Framework NANOMOF project under grant agreement CP-IP 228604-2.

C.L. acknowledges the Mega-grant of the Russian Federation Government to support scientific research at Southern Federal University, No. 14.Y26.31.0001.

References

[1] R. Yan, T. Chin, Y. L. Ng, H. Duan, D. T. Liang, J. H. Tay, Environ. Sci. Technol. 38 (2004) 316-323.

[2] W. Yuan, T. J. Bandosz, Fuel 86 (2007) 2736-2746.

[3] X. Wang, X. Ma, X. Xu, L. Sun, C. Song, Top. Catal. 49 (2008) 108-117.

[4] G. Ferey, C. Serre, T. Devic, G. Maurin, H. Jobic, P. L. Llewellyn, G. De Weireld, A. Vimont, M. Daturi, J. S. Chang, Chem. Soc. Rev. 40 (2011) 550-562.

[5] H. Furukawa, K. E. Cordova, M. O'Keeffe, O. M. Yaghi, Science 341 (2013) 1230441-1230441.

[6] L. Hamon, H. Leclerc, A. Ghoufi, L. Oliviero, A. Travert, J.-C. Lavalley, T. Devic, C. Serre, G. Ferey, G. De Weireld, A. Vimont, G. Maurin, J. Phys. Chem. C 115 (2011) 2047-2056.

[7] L. Hamon, C. Serre, T. Devic, T. Loiseau, F. Millange, G. Ferey, G. De Weireld, J. Am. Chem. Soc. 131 (2009) 8775-8777.

[8] A. Peluso, N. Gargiulo, P. Aprea, F. Pepe, D. Caputo, Sci. Adv. Mater. 6 (2014) 164-170.

[9] S. Chavan, F. Bonino, L. Valenzano, B. Civalleri, C. Lamberti, N. Acerbi, J. H. Cavka, M. Leistner, S. Bordiga, J. Phys. Chem. C 117 (2013) 15615-15622.

[10] T. Devic, G. De Weireld, G. Ferey, L. Hamon, T. Loiseau, C. Serre, Polytechnique De Mons; Cent Nat Rech Sci; Cnrs Cent Nat Rech Sci; Univ Mons.

[11] S. S. Y. Chui, S. M. F. Lo, J. P. H. Charmant, A. G. Orpen, I. D. Williams, Science 283 (1999) 1148-1150.

[12] C. Prestipino, L. Regli, J. G. Vitillo, F. Bonino, A. Damin, C. Lamberti, A. Zecchina, P. L. Solari, K. O. Kongshaug, S. Bordiga, Chem. Mat. 18 (2006) 1337-1346.

[13] S. Bordiga, L. Regli, F. Bonino, E. Groppo, C. Lamberti, B. Xiao, P. S. Wheatley, R. E. Morris, A. Zecchina, Phys. Chem. Chem. Phys. 9 (2007) 2676-2685.

[14] K. S. Lin, A. K. Adhikari, C. N. Ku, C. L. Chiang, H. Kuo, Int. J. Hydrog. Energy 37 (2012) 13865-13871.

[15] E. Borfecchia, S. Maurelli, D. Gianolio, E. Groppo, M. Chiesa, F. Bonino, C. Lamberti, J. Phys. Chem. C 116 (2012) 19839-19850.

[16] B. Supronowicz, A. Mavrandonakis, T. Heine, J. Phys. Chem. C 117 (2013) 14570-14578.

[17] C. Petit, B. Mendoza, T. J. Bandosz, ChemPhysChem 11 (2010) 3678-3684.

[18] C. Petit, T. J. Bandosz, Dalton Trans. 41 (2012) 4027-4035.

[19] C. Petit, B. Levasseur, B. Mendoza, T. J. Bandosz, Microporous Mesoporous Mater. 154 (2012) 107-112.

[20] J. J. Gutierrez-Sevillano, A. Martin-Calvo, D. Dubbeldam, S. Calero, S. Hamad, RSC Adv. 3 (2013) 14737-14749.

[21] X. C. Huang, Y. Y. Lin, J. P. Zhang, X. M. Chen, Angew. Chem.-Int. Edit. 45 (2006) 1557-1559.

[22] W. Morris, C. J. Stevens, R. E. Taylor, C. Dybowski, O. M. Yaghi, M. A. Garcia-Garibay, J. Phys. Chem. C 116 (2012) 13307-13312.

[23] Y. Hu, H. Kazemian, S. Rohani, Y. N. Huang, Y. Song, Chem. Commun. 47 (2011) 12694-12696.

[24] L. H. Wee, T. Lescouet, J. Ethiraj, F. Bonino, R. Vidruk, E. Garrier, D. Packet, S. Bordiga, D. Farrusseng, M. Herskowitz, J. A. Martens, ChemCatChem 5 (2013) 3562-3566.

[25] H. Li, X. Feng, Y. Guo, D. Chen, R. Li, X. Ren, X. Jiang, Y. Dong, B. Wang, Scientific Reports 4 (2014) 4366.

[26] F. Bonino, C. Lamberti, S. Chavan, J. G. Vitillo, S. Bordiga, in Metal Organic Frameworks as Heterogeneous Catalysts (Eds.: F. X. Llabres i Xamena, J. Gascon), The Royal Society of Chemistry, Cambridge, (2013, ch. 4), pp. 76-142.

[27] E. Borfecchia, D. Gianolio, G. Agostini, S. Bordiga, C. Lamberti, in Metal Organic Frameworks as Heterogeneous Catalysts (Eds.: F. X. Llabres i Xamena, J. Gascon), The Royal Society of Chemistry, Cambridge, (2013, ch. 5), pp. 143-208.

[28] S. Bordiga, F. Bonino, K. P. Lillerud, C. Lamberti, Chem. Soc. Rev. 39 (2010) 4885-4927.

[29] J. Alvarez-Garcia, E. Rudigier, N. Rega, B. Barcones, R. Scheer, A. Perez-Rodriguez, A. Romano-Rodriguez, J. R. Morante, Thin Solid Films 431 (2003) 122-125.

[30] G. Kumari, K. Jayaramulu, T. K. Maji, C. Narayana, J. Phys. Chem. A 117 (2013) 11006-11012.

[31] K. Tezuka, W. C. Sheets, R. Kurihara, Y. J. Shan, H. Imoto, T. J. Marks, K. R. Poeppelmeier, Solid State Sciences 9 (2007) 95-99.

Figure Captions

Figure 1. a) FT-IR spectra of in air (cyan curve) and activated at 423K for 1h (blue curve) HKUST-1; b) FT-IR spectra of in air (dark grey) and activated at 573K for 2h (black curve) ZIF-8.

Figure 2. FT-IR spectra reporting increasing adsorption dosages of H_2S (from grey to olive/dark yellow curves) on activated HKUST-1 (part a) blue curve) and ZIF-8 (part b) black curve).

Figure 3. Raman spectra of a): in air (cyan curve), activated (blue curve) and interacting with H_2S (olive curves) HKUST-1 (λ =514 nm); b): in air (grey curve) and activated (black curve) ZIF-8 (λ=785 nm).

Figure 4. Part a1) and b1) images corresponding to HKUST-1 and ZIF-8 in air, activated and interacting with H_2S. DRUV-Vis-NIR spectra of HKUST-1 (part a2)) in air (cyan curve), activated (blue curve) and interacting with H_2S (grey and olive curves) and of ZIF-8 (part b2)) in air (grey curve), activated (black curve) and interacting with H_2S (dark yellow curve).

Figure 5. PXRD patterns of HKUST-1 in air and after interaction with H_2S (part a), cyan and olive curves) and ZIF-8 (part b), grey and dark yellow curves). Reflections labelled with full circles represent new phases.

Figures

Figure 1.

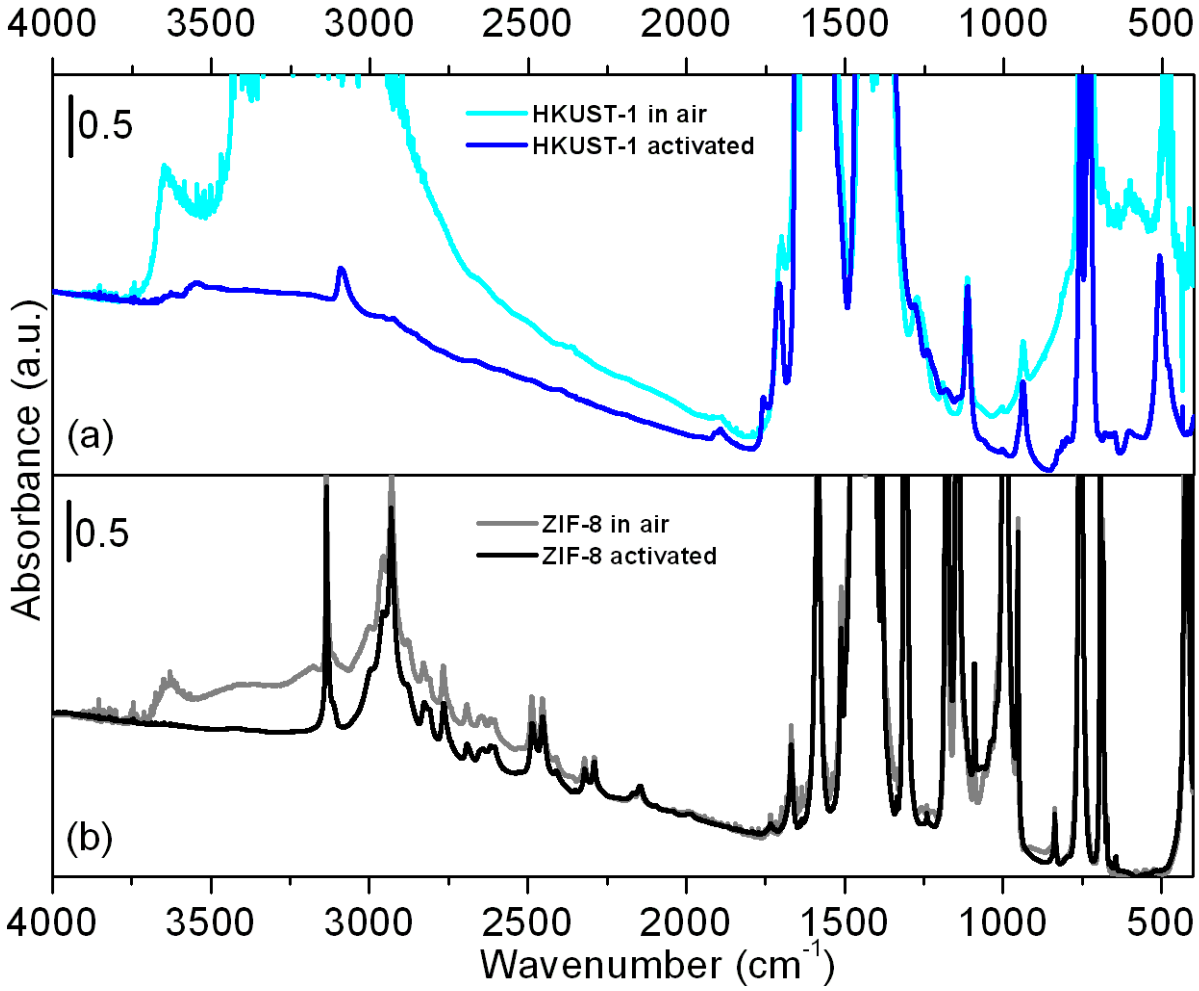

Figure 2.

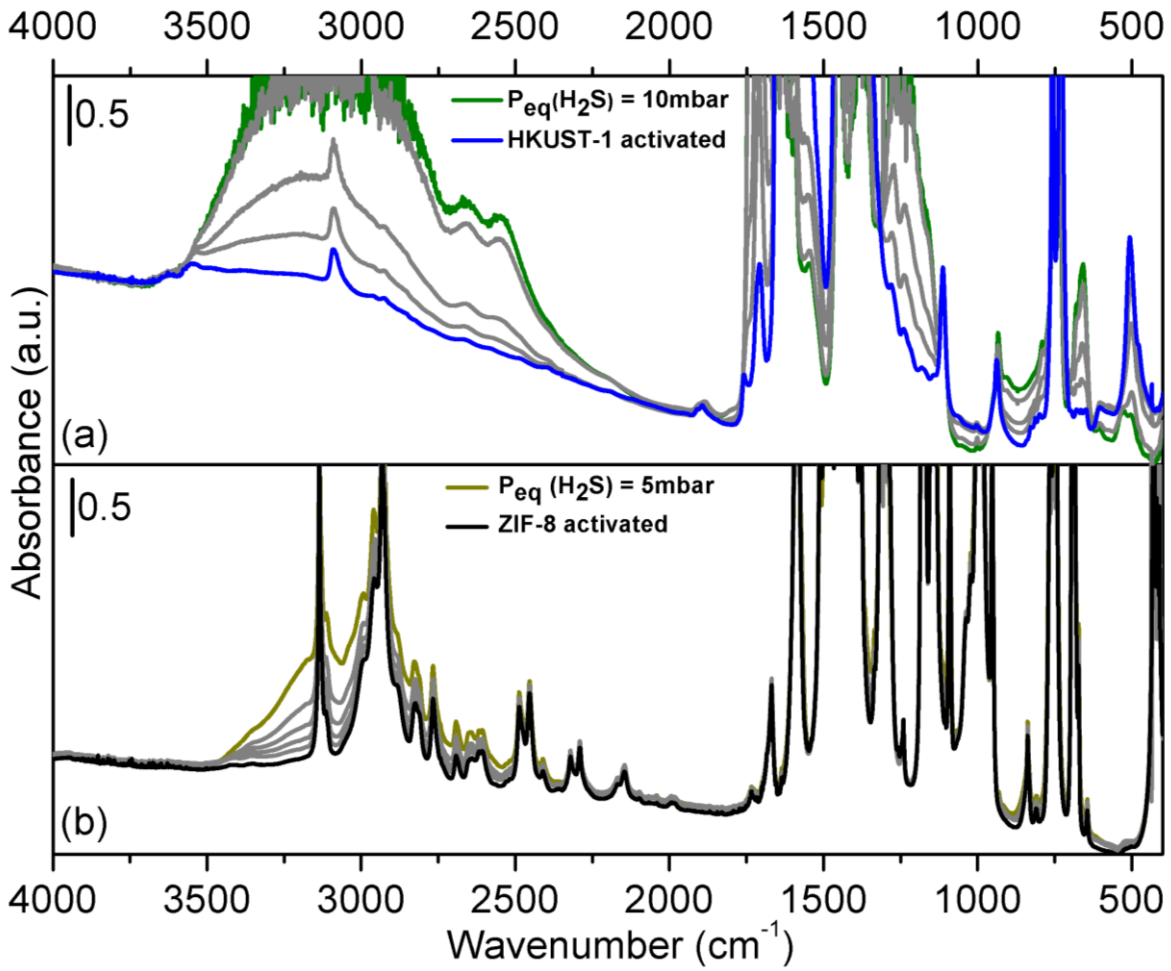
4000
3500
3000
2500
2000
1500
1000
500
0.5
$P_{eq}(H_2S)$ = 10mbar
HKUST-1 activated
(a)
0.5
P_{eq} (H_2S) = 5mbar
ZIF-8 activated
(b)
Absorbance (a.u.)
Wavenumber (cm^{-1})

Figure 3.

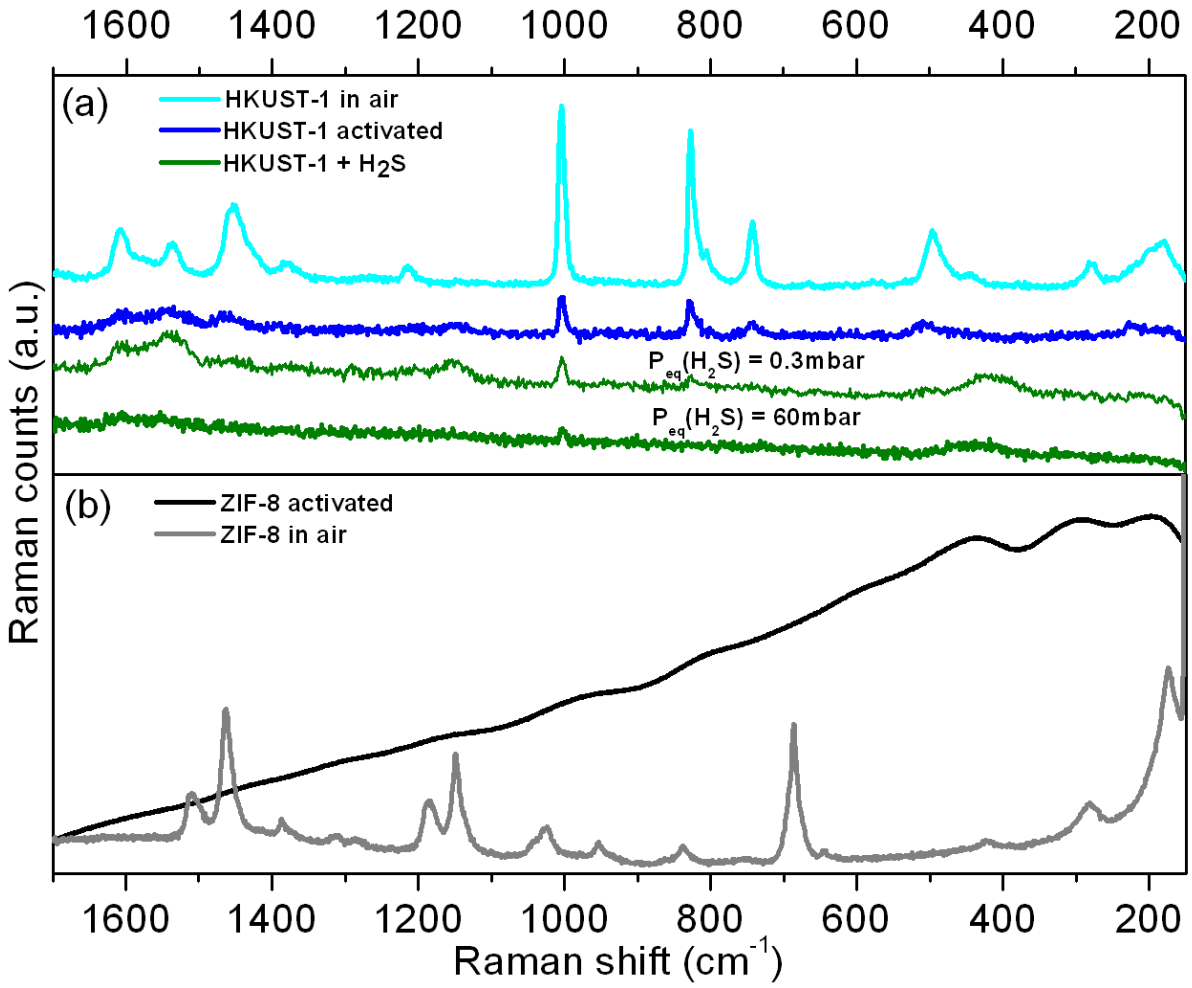
1600
1400
1200
1000
800
600
400
200
(a)
HKUST-1 in air
HKUST-1 activated
HKUST-1 + H2S
Peq(H2S) = 0.3mbar
Peq(H2S) = 60mbar
(b)
ZIF-8 activated
ZIF-8 in air
Raman counts (a.u.)
Raman shift (cm-1)

Figure 4.

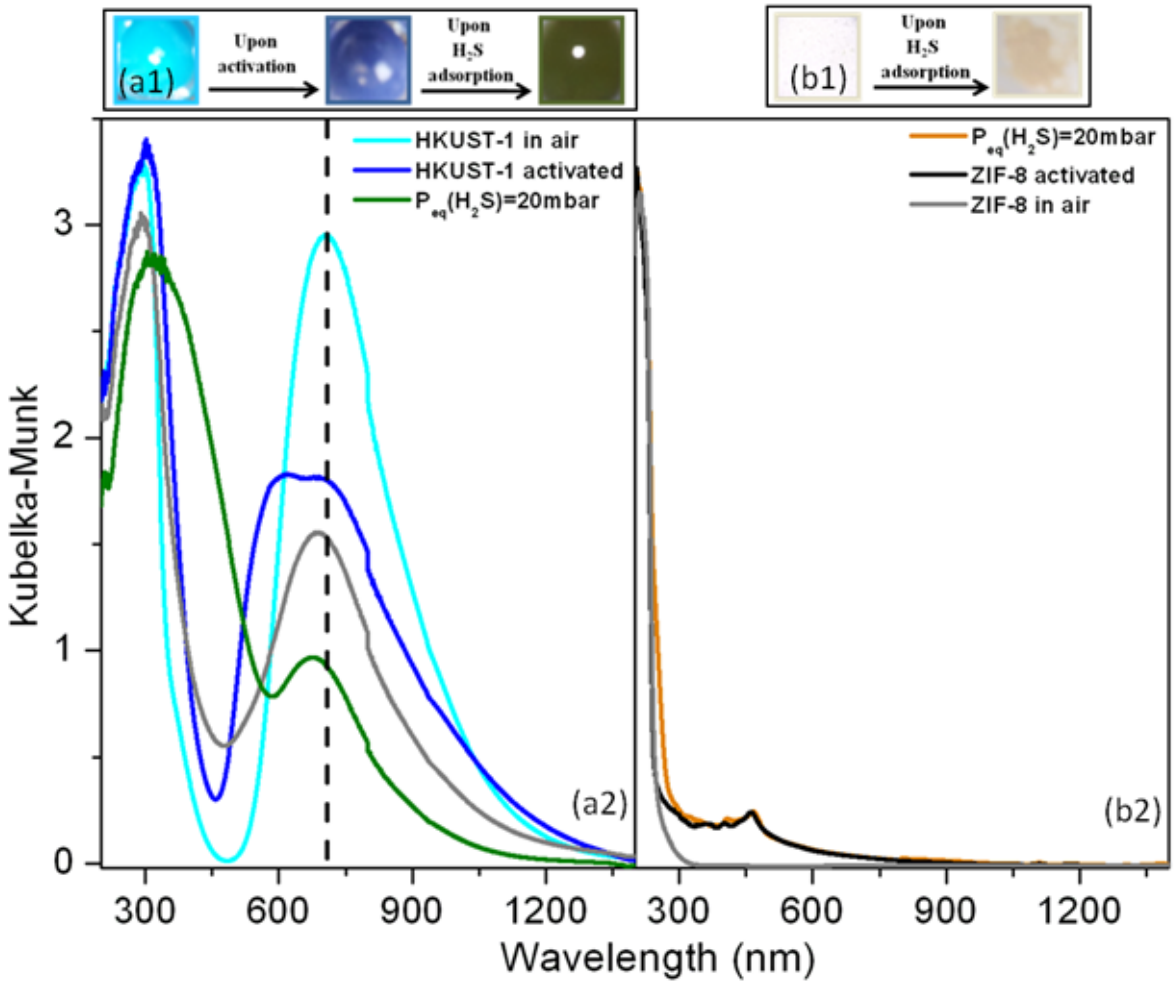
(a1)
Upon activation
Upon H_2S adsorption
(b1)
Upon H_2S adsorption
HKUST-1 in air
HKUST-1 activated
$P_{eq}(H_2S)$=20mbar
$P_{eq}(H_2S)$=20mbar
ZIF-8 activated
ZIF-8 in air
Kubelka-Munk
0
1
2
3
(a2)
(b2)
300
600
900
1200
300
600
900
1200
Wavelength (nm)

Figure 5.

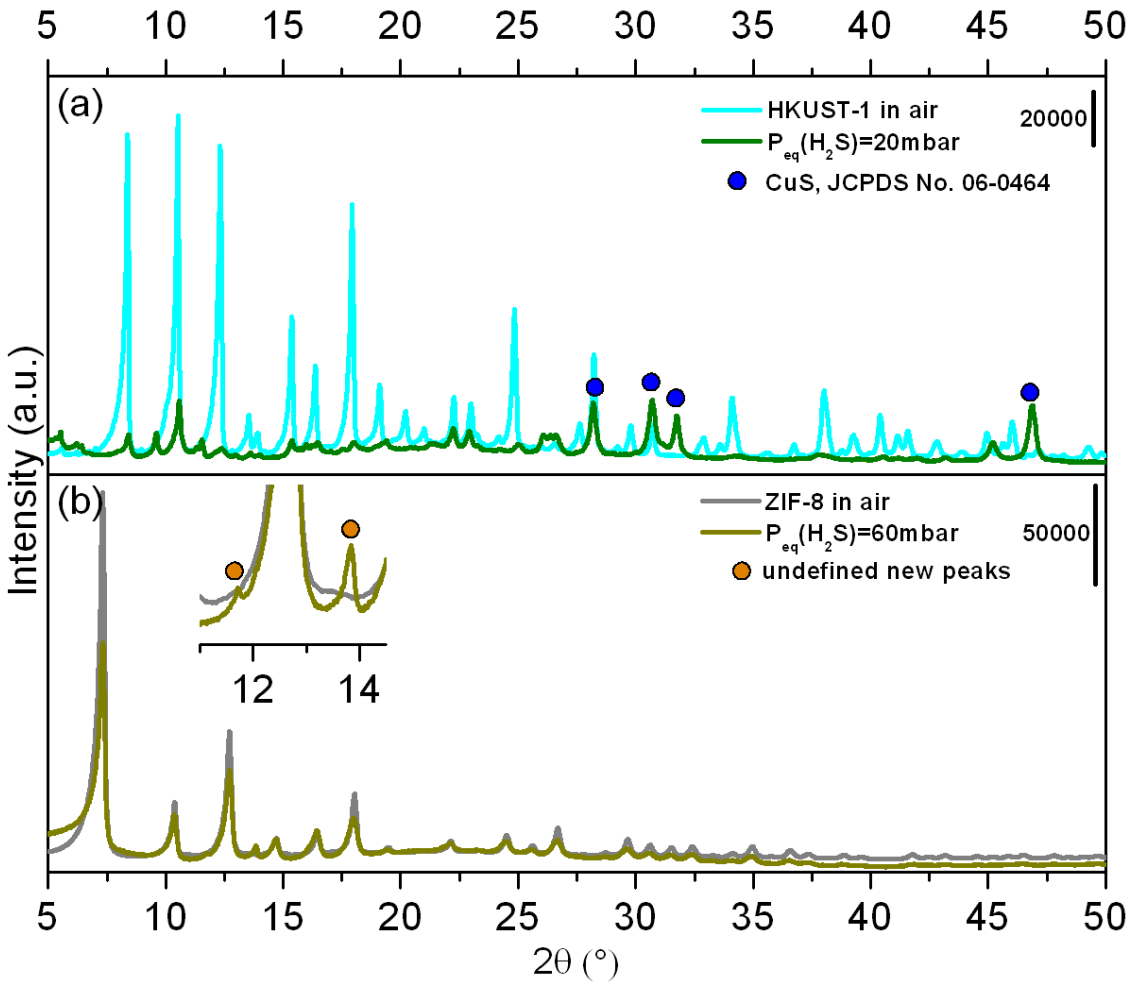
(a)
HKUST-1 in air
$P_{eq}(H_2S)$=20mbar
CuS, JCPDS No. 06-0464
20000
(b)
ZIF-8 in air
$P_{eq}(H_2S)$=60mbar
undefined new peaks
50000
12
14
Intensity (a.u.)
2θ (°)
5
10
15
20
25
30
35
40
45
50